Proceedings of 12th Cambridge Workshop on Cool Stars, Stellar Systems, & The Sun, 2003 University of Colorado.

Shock Formation and Energy Dissipation of Slow Magnetosonic Waves in Coronal Plumes

M. Cuntz[1], S. T. Suess[2]

Abstract.

We study the shock formation and energy dissipation of slow magnetosonic waves in coronal plumes. The wave parameters and the spreading function of the plumes as well as the base magnetic field strength are given by empirical constraints mostly from SOHO/UVCS. Our models show that shock formation occurs at low coronal heights, i.e., within 1.3 $R_\odot$, depending on the model parameters. In addition, following analytical estimates, we show that scale height of energy dissipation by the shocks ranges between 0.15 and 0.45 $R_\odot$. This implies that shock heating by slow magnetosonic waves is relevant at most heights, even though this type of waves is apparently not a solely operating energy supply mechanism.

1. Introduction

Plumes are bright quasi-radial rays in coronal holes, visible between one and several solar radii as found by the Ultraviolet Coronograph Spectrometer (UVCS), the Large-Angle and Spectrometric Coronograph (LASCO), and the Extreme Ultraviolet Imaging Telescope (EIT) on the Solar and Heliospheric Observatory (SOHO) (e.g., DeForest et al. 1997) as well as by other space instruments and ground-based observations. Plumes lie over photospheric magnetic flux concentrations, although not all flux concentrations have plumes. Plumes are of low-β plasma and are considered to be in pressure balance with the ambient medium.

There is continuing interest in plumes precisely because they (1) are a tracer of structures in the corona, (2) contribute to the mass and energy balance of the solar wind, and (3) exhibit a range of interesting dynamic phenomena. Observations of polar plumes led to the detection of quasi-periodic density variations (Ofman et al. 1997, 2000; DeForest & Gurman 1998), which were identified through quasi-periodic perturbations in the brightness of Fe IX and Fe X line emission near 171 Å. These intensity fluctuations are now interpreted as slow magnetosonic waves with periods of 10-15 min and propagation speeds of 75-150 km s^{-1} (DeForest & Gurman 1998; Ofman et al. 1999). These waves are expected to contribute to the heating and wind acceleration within the plumes, which is relevant to the overall plume dynamics.

---

[1]Department of Physics, University of Texas at Arlington

[2]Space Science Laboratory, NASA Marshall Space Flight Center

In this paper, we discuss the shock formation and energy dissipation of slow magnetosonic waves in solar plumes. The formation of shocks is calculated based on the characteristic physical properties of plumes including heat conduction, radiative damping, and plume spreading calculated following Suess (1998) and Suess et al. (1998). The energy dissipation length of the waves also depends on the carry-along effect of the solar wind, initiated by a secondary heating mechanism (e.g., Alfvén waves).

2. Calculation of Wave Models

The wave models are calculated based on the modified method of characteristics, which has already been used for the computation of longitudinal chromospheric flux tube models for the Sun (e.g., Herbold et al. 1985) and other types of stars (e.g., Cuntz et al. 1999). In this case, the waves are followed to the point of shock formation and beyond. An important aspect of chromospheric flux tube as well as coronal plume models is the role of the area function $A(r)$, which invokes the dilution (or concentration) of the wave energy flux as function of height. Previous models have shown (Fawzy et al. 1998) that different values of $A(r)$ lead to height-dependent differences in the wave heating and also affect the height of shock formation. In spherical coordinates, we take

$$A(r) \;=\; A_{\rm o} \left(\frac{r}{r_{\rm o}}\right)^2 f(r) \tag{1}$$

with $f(r)$ as spreading factor and $A_{\rm o} f(r_{\rm o})$ as the area of the plume at its base, i.e., at radius $r_{\rm o}$. The magnetic field strength inside of plumes follows from the conservation of the magnetic flux density ϕ given by $\phi = A(r)B(r) = A_{\rm o} f(r_{\rm o}) B_{\rm o}$ with $B_{\rm o}$ as magnetic field strength at the base.

Theoretical predictions for $f(r)$ for coronal plumes were given by Suess (1998) and Suess et al. (1998). They assumed that the plume spreading can be considered as consisting of two parts, i.e. the *local* spreading $f_l(r)$ and the *global* spreading $f_g(r)$ with $f(r)$ mathematically given by $f(r) = f_l(r) f_g(r)$. The local spreading $f_l(r)$ is important below 35,000 km, varies rapidly at these heights, and is constant above that height. On the other hand, $f_g(r)$ varies much more slowly at those heights. Suess et al. found that the geometrical spreading of plumes can be computed with acceptable accuracy independent of the flow because $\beta \ll 1$ in plumes and throughout the surrounding coronal holes from the base of the corona to at least 10 $R_\odot$. Conversely, the global spreading $f_g(r)$ can be computed from a global model of the corona (Wang et al. 1998). It is found that the behavior of $f_g(r)$ is largely given by the coronal hole geometry, which can either be estimated empirically or theoretically from the study of MHD models. Following Suess et al. (1998), it is found that

$$f_l(r) \;=\; 1 + 13.31 \cdot \left(1 - e^{-\frac{r/R_\odot - 1}{0.011}}\right) \tag{2}$$

and

$$f_g(r) \;=\; a_0 + a_1 \frac{r}{R_\odot} + a_2 \left(\frac{r}{R_\odot}\right)^2 + a_3 \left(\frac{r}{R_\odot}\right)^3 + a_4 \left(\frac{r}{R_\odot}\right)^4 \tag{3}$$

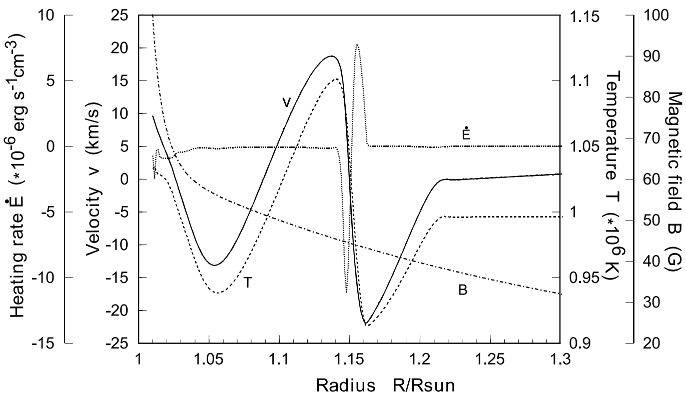

Figure 1. Snapshot of a slow magnetosonic wave with a period of 10 min and an initial amplitude of 0.10 Mach in a solar coronal plume after 970 s. Shown are: the flow speed v (*solid line*), temperature T (*dashed line*), magnetic field strength B (*dashed-dotted line*), and the thermal heating rate $\dot{E}$ (*dotted line*), which is almost entirely determined by heat conduction.

with $R_\odot$ as solar radius, and $a_0 = 0.24974$, $a_1 = 0.76714$, $a_2 = -0.085164$, $a_3 = 0.0093196$, and $a_4 = -0.0004403$. These numbers are for a typical plume base field strength of 20 times the interplume field and a large coronal hole. They give $f_l \simeq 14$ at 1.2 $R_\odot$ and $f_g \simeq 2.8$ and $f \simeq 41$ at 5 $R_\odot$.

In our models we assume a single-fluid medium with a temperature of $T = 10^6$ K. The initial density model follows the solution of the wind equation with $v_{w\text{o}} = 0.15$ km s^{-1} and $N_{H\text{o}} = 1.2 \times 10^8$ cm^{-3} at $r_\text{o} = 1.01 R_\odot$, where $v_{w\text{o}}$ and $N_{H\text{o}}$ are the wind speed and hydrogen number density, respectively. At radius r_o, we assume a magnetic field strength of $B_\text{o} = 100$ G and a plume opening radius of 1000 km. Our models also consider radiative damping and heat conduction. Radiative damping is found to be relative unimportant for the energetics of the shocks, owing to the low coronal densities. Heat conduction, however, is found to reduce the temperature jumps of the shocks, resulting in changes of the dynamic structure of the shock wave patterns.

3. Shock Formation

The formation of shocks is calculated using the well-established "wave braking criterion" (e.g., Courant & Friedrichs 1976), which defines shock formation based on the turn-over of the wave profile. This leads to changes in the wave profile until the density function is no longer single valued. Mathematically, shock formation is found when two C$^+$ characteristics intersect in the space-time plane. This criterion has already been used in numerous studies of acoustic (e.g., Stein & Schwartz 1972; Ulmschneider et al. 1977) and magnetic wave propagation (e.g., Herbold et al. 1985; Fawzy et al. 1998; Cuntz et al. 1999). For longitudinal waves in an Eulerian coordinate system the slope of C$^+$ characteristics is given by $c_T + v$ with c_T as tube speed and v as flow speed encompassing both the wave and the ambient flow speed of the wind. The tube speed c_T is always lower than the adiabatic sound speed c_S with the exact difference expressible through plasma-β (e.g., Cuntz 1999).

We now focus on the structure of our time-dependent MHD wave models. At the inner boundary of the models, i.e. at radius $r_o = 1.01 R_\odot$, slow magnetosonic waves are introduced assuming a sinusoidal wave profile. These waves are followed up to the point of shock formation. Due to the changes of the density as function of height, the waves encounter nonlinear steepening and a distortion of the wave profile. Figure 1 shows a snapshot of a wave with a period of 10 min and an initial amplitude of 0.10 Mach, corresponding to a wave energy flux of 4.1×10^3 ergs cm^{-2} s^{-1}. Here the wave amplitude has increased from Δv = 14.2 to 20.3 km s^{-1}. The wave model also shows temperature fluctuations as function of height, as expected. The snapshot has been taken at an elapsed time of 970 s, shortly before shock formation, occurring at 1007.7 s. Shock formation is found at 1.16 $R_\odot$, corresponding to a distance of 1.2 wavelengths. Figure 1 also depicts the behavior of the heating rate $\dot{E}$ (or cooling rate if $\dot{E} < 0$) given by the joint influence of heat conduction and the loss of radiative energy. It is found that $\dot{E}$ is positive in the compression zone of the wave ($v > 0$, $T > \bar{T}$) and negative in the depression zone ($v < 0$, $T < \bar{T}$, with $\bar{T}$ as mean temperature). The behavior of $\dot{E}$ is almost entirely given by heat conduction, and therefore $\dot{E}$ is found to be double-peaked, concentrated near the region of shock formation.

4. Effects of Plume Geometry, Wave Parameters and the Solar Wind

In order to obtain further insight into the formation of shocks, we consider a grid of models with different wave parameters, with and without plume geometry and with and without inclusion of the solar wind. We consider wave periods between 10 and 15 min (DeForest & Gurman 1998) and initial wave amplitudes of 0.05 and 0.2 Mach (7.1 and 28.3 km s^{-1}, respectively). This choice is motivated by empirical estimates of wave amplitudes ranging between Δv = 7.5 km s^{-1} (Ofman et al. 1999) and Δv = 15 km s^{-1} (DeForest & Gurman 1998). In addition, we also consider waves of larger amplitudes. Ofman et al. estimated that slow magnetosonic waves are expected to provide between 0.02 and 0.30 of the total energy required to heat and accelerate the fast solar wind. Following Cuntz & Suess (2001), the shock formation height is found to be lowest for large amplitude and short period waves. For $P = 10$ min, the shock formation height decreases from 1.26 $R_\odot$ to 1.09 $R_\odot$ if the initial wave amplitude is increased from 0.05 to 0.20 Mach. For $P = 15$ min, the height of shock formation decreases from 1.32 $R_\odot$ to 1.12 $R_\odot$ for the same range of initial amplitudes.

A further topic of interest is the study of the influence of the solar wind on the damping length of the wave energy flux. Figure 2 shows a variety of theoretical models, which differ regarding the selected wave amplitude, wave period and inclusion of the wind. As amplitudes, we have taken 7.5 and 15.0 km s^{-1} (Ofman et al. 1999), corresponding to shock strength of $M_s = 1.07$ and 1.14, respectively, which efficiently ensures that the weak shock approximation is applicable. In the models calculated, following the method given by Cuntz et al. (2002) and Cuntz & Suess (2002), it is found that the wave energy damping length ranges between 0.15 $R_\odot$ and 0.45 $R_\odot$, and furthermore increases as function of height. For wave models with periods of 10 min, we also studied

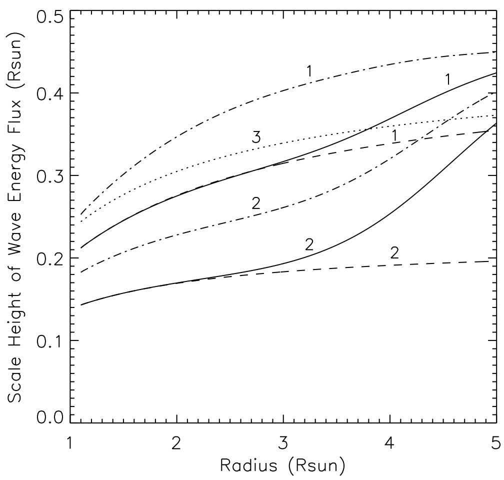

Figure 2. Wave energy damping length for a variety of models. We show two sets of curves consisting of three lines each, belonging to the following models: plume geometry without wind, $P = 10$ min (dashed lines) and plume geometry with wind, $P = 10$ min (solid lines) and $P = 15$ min (dashed-dotted lines). For the upper set of curves (1), the wave amplitudes are 7.5 km s^{-1}, whereas for the lower set of curves (2) they are 15 km s^{-1} instead. For comparison, we also show the case of spherical symmetry, no wind, for waves of $P = 10$ min and 7.5 km s^{-1} (dotted line), see curve (3).

the role of the solar wind in the spatial increase of the wave energy damping length in particular detail. We found that the cases with wind and without wind were virtually identical below 2.3 $R_\odot$ for $M_s = 1.14$ and below 3.1 $R_\odot$ for $M_s = 1.07$. However, at larger heights, the wave energy damping lengths in models with wind are increased compared to models without wind. At radius 5 $R_\odot$, the increase of the wave energy damping length in the $M_s = 1.07$ model is found to be 20%, whereas in the $M_s = 1.14$ model, it is found to be as large as 85%. This shows that the "carry-along effect" of the wind is of pivotal importance for the energy dissipation of the waves. The carry-along effect of the wind efficiently offsets the dilution of the wave energy by the plume geometry given by the increase of the spreading with height.

5. Conclusions

We explored the height of shock formation of slow magnetosonic waves in coronal plumes and deduced estimates for the scale height of wave energy dissipation by analytical means. Our models take into account plume geometric spreading, heat conduction and radiative damping. As wave parameters, we consider periods between 10 and 15 min (DeForest & Gurman 1998), with initial wave amplitudes between 0.05 and 0.2 Mach (7.1 and 28.3 km s^{-1}, respectively). We found the following results:

(1) Shock formation occurs at low coronal heights, i.e., within 1.3 $R_\odot$, depending on the model parameters. The shock formation height is lowest for large amplitude waves and waves with relatively short periods.

(2) Shock formation is significantly affected by the large plume basal spreading. Owing to the dilution of the wave energy flux, larger spreading close to the plume base increases the height where shock are formed.

(3) The damping length of the wave energy flux ranges between 0.15 and 0.45 $R_\odot$, commensurate with empirical energy requirements. This shows that energy dissipation by slow magnetosonic waves is relevant at most heights, although these waves are apparently not a solely operating energy supply mechanism.

(4) The damping length of the wave energy flux increases up to 85% through the "carry-along effect" of the solar wind. This effect is found to be largest for high-amplitude waves. The carry-along effect of the wind efficiently offsets the dilution of the wave energy by the plume geometry given by the increase of the spreading with height.

Acknowledgments. This work has been supported by the UAH/USRA/ NASA Cooperative Agreement for Research in Space Plasma Physics (M.C.) and by the Ulysses/SWOOPS experiment team (S.T.S.).

References

Courant, R., & Friedrichs, K.O. 1976, Supersonic Flow and Shock Waves, Springer, New York

Cuntz, M. 1999, A&A, 350, 1100

Cuntz, M., Rammacher, W., Ulmschneider, P., Musielak, Z.E., & Saar, S.H. 1999, ApJ, 522, 1053

Cuntz, M., Suess, S.T. 2001, ApJ, 549, L143

Cuntz, M., Suess, S.T. 2002, A&A, submitted

Cuntz, M. Ulmschneider, P., Rossi, P. 2002, A&A, submitted

DeForest, C.E., et al. 1997, Solar Phys.., 175, 393

DeForest, C.E., & Gurman, J.B. 1998, ApJ, 501, L217

Fawzy, D.E., Ulmschneider, P., & Cuntz, M. 1998, A&A, 336, 1029

Herbold, G., Ulmschneider, P., Spruit, H.C., & Rosner, R. 1985, A&A, 145, 157

Ofman, L., Nakariakov, V.M., & DeForest, C.E. 1999, ApJ, 514, 441

Ofman, L., Romoli, M., Poletto, G., Noci, G., & Kohl, J.L. 1997, ApJ, 491, L111 (erratum 507, L189 [1998])

Ofman, L., Romoli, M., Poletto, G., Noci, G., & Kohl, J.L. 2000, ApJ, 529, 592

Stein, R.F., & Schwartz, R.A. 1972, ApJ, 177, 807

Suess, S.T. 1998, in *Solar Jets and Coronal Plumes*, ESA-SP-421, p. 223

Suess, S.T., Poletto, G., Wang, A.-H., Wu, S.T., & Cuseri, I. 1998, Solar Phys., 180, 231

Ulmschneider, P., Kalkofen, W., Nowak, T., & Bohn U. 1977, A&A, 54, 61

Wang, A.H., Wu, S.T., Suess, S.T., & Poletto, G. 1998, J. Geophys. Res., 103 (2), 1913